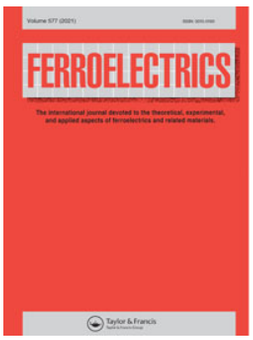

Ferroelectrics

ISSN: (Print) (Online) Journal homepage: https://www.tandfonline.com/loi/gfer20

Synthesis and luminescence properties of chemically synthesized ZnS nanomaterials

B. Sreenivasulu, B. Rama Sagar, S. Venkatramana Reddy & B. Sankara Reddy

To cite this article: B. Sreenivasulu, B. Rama Sagar, S. Venkatramana Reddy & B. Sankara Reddy (2021) Synthesis and luminescence properties of chemically synthesized ZnS nanomaterials, Ferroelectrics, 577:1, 91-98, DOI: 10.1080/00150193.2021.1916353

To link to this article: https://doi.org/10.1080/00150193.2021.1916353

Published online: 30 Jun 2021.

Submit your article to this journal

View related articles

View Crossmark data

Full Terms & Conditions of access and use can be found at
https://www.tandfonline.com/action/journalInformation?journalCode=gfer20

FERROELECTRICS
2021, VOL. 577, 91–98
https://doi.org/10.1080/00150193.2021.1916353

Taylor & Francis
Taylor & Francis Group

Check for updates

Synthesis and luminescence properties of chemically synthesized ZnS nanomaterials

B. Sreenivasulu[a], B. Rama Sagar[b], S. Venkatramana Reddy[c], and B. Sankara Reddy[c]

[a]Department of Physics, Annamacharya Institute of Technology & Sciences (Autonomous), Rajampet, Andhra Pradesh, India; [b]Department of Physics, Govt. Degree College, Rayachoty, Andhra Pradesh, India; [c]Department of Physics, Sri Venkateswara University, Tirupati, Andhra Pradesh, India

ABSTRACT

Pure and Cu-doped ZnS nanomaterials were successfully synthesized at room temperature by the chemical co-precipitation method. X-ray diffraction (XRD) pattern shows that the synthesized nanomaterials have a cubic blended structure, and the size of crystallites is around 2–3 nm. These results were confirmed by transmission electron microscopy (TEM), which matched well with the XRD results. Scanning electron microscopy and TEM micrographs of ZnS nanomaterials were in spherical shaped nature. The chemical composition is found in pure and doped ZnS nanomaterials using EDAX spectra. UV-Vis spectra show the absorption peak between 310 and 320 nm. Photoluminescence studies reveal sharp emission peaks at 439, 450 and 466 nm with decreasing intensity for pure and doped nanomaterials.

ARTICLE HISTORY
Received 22 August 2020
Accepted 4 March 2021

KEYWORDS
ZnS nanopowders; XRD; SEM with EDAX; absorption spectra; PL and HR-TEM

1. Introduction

Dilute magnetic semiconductors (DMSs) have been an active field of research due to their novel properties that allow the control of both the spin and charge of carriers [1], which can be used as effective platforms for biomedical imaging, drug delivery, protein separation and MRI contrast imaging [2–5]. Zinc sulfide, a typical II–VI compound semiconductor, with a direct band gap of 3.67 eV at room temperature and 40 meV as exaction binding energy. It is a very good semiconductor material used in displays, sensors and lasers [6–8]. Great progress had been achieved in realizing the optical and magnetic properties simply by changing the doped ions in zinc sulfide nanoparticles. Among these doped ions, ZnS: TM^{2+} (TM = transition metals) nanoparticles have been regarded as a promising new class of DMS with their superior color-tunable emission and magnetic properties [9–11]. Upon excitation, the ZnS: (Cu, Ni) co-doped nanoparticles show blue and green emissions centered at 460 and 520 nm [12]; the ZnS: Fe^{2+} and ZnS:Mn^{2+} Fe^{2+} nanomaterials show ferromagnetism around room temperature [13, 14], co-doped ZnS quantum dots with their excellent luminescent properties have potential applications in LEDs, plasma displays, sensors and lasers [15]. Recently, Park et al. [16] have tried to apply the ZnS:Mn, Cu and Cl phosphors for the EL device. Such phosphors have several excellent features, including

CONTACT S. Venkatramana Reddy drsvreddy123@gmail.com
© 2021 Taylor & Francis Group, LLC

spectral adjustable, high quantum efficiency and photostability. Since Cu is a non-magnetic element, the 3d orbital in Cu ($3d^{10}4s^1$) is fully filled and hence does not contribute to the ferromagnetism. Moreover, its secondary phases, such as CuS display antiferromagnetism, and Cu_2S shows no magnetism due to the fully filled 3d orbitals [17]. Up to now, the issue about the origin of the ferromagnetism properties of the ZnS: (Cu, Ni) co-doped nanomaterials have been still blurry. In the past few years, several techniques have been employed to synthesize the ZnS: Cu^{2+} nanoparticles, such as precipitation, solvo thermal and thermal co-evaporation at high temperature [18–20].

In the present work, a simple soft chemical method, namely chemical co-precipitation method for the synthesis of un-doped and PVP-encapsulated ZnS: Cu-doped nanoparticles is presented. This method is adopted because it is a low cost, and the dopant concentration can be easily attained. Structural, compositional, morphological and optical studies of the prepared samples are carried out by X-ray diffraction (XRD), energy dispersive X-ray spectroscopy (EDS), scanning electron microscopy (SEM), transition electron microscopy (TEM), HR-TEM, selected area electron diffraction (SAED), UV-visible spectroscopy (UV-Vis), photoluminescence (PL).

2. Experimental

2.1. Synthesis of powders

Pure and Cu-doped Zinc sulfide nanopowders were synthesized with a chemical method with zinc acetate, copper acetate tetra hydrate and sodium sulfide were used for powders preparation. [Zn $(CH_3COO)_2$. $2H_2O$] is dissolved in double-distilled water, and then Na_2S aqueous solution is also added to the above solution drop-by-drop under constant magnetic stirring. After 3 min, a white precipitate is formed. By adding of [Cu $(CH_3COO)_2$. $4H_2O$] to the above precipitate with continuous magnetic stirring, Cu-doped ZnS nanopowders were obtained. PVP capping agent is used to stabilize the ZnS nanopowders. The precipitate is washed several times with doubled-distilled water and filtered out. The precipitate is dried at 80 °C for 9 h, further characterization of the samples.

2.2. Characterization

Synthesized nanoparticles are carefully characterized under mentioned characterization studies. Powder XRD pattern is recorded with Bruker diffractometer between 10 and 90° range, using Cu Kα source of wavelength $\lambda = 1.53906$ Å. The UV–Vis diffusion reflectance spectroscopy used to study optical properties and is in the wavelength range of 200–3000 nm. Photoluminescence properties are carried out with FLS-980 spectrometer. The chemical composition and surface morphology of pure and doped ZnS nanoparticles are investigated by EDAX and SEM. TEM and SAED are recorded on a Technai G20-Stwin and HRTEM accelerating with a voltage of 250 kV.

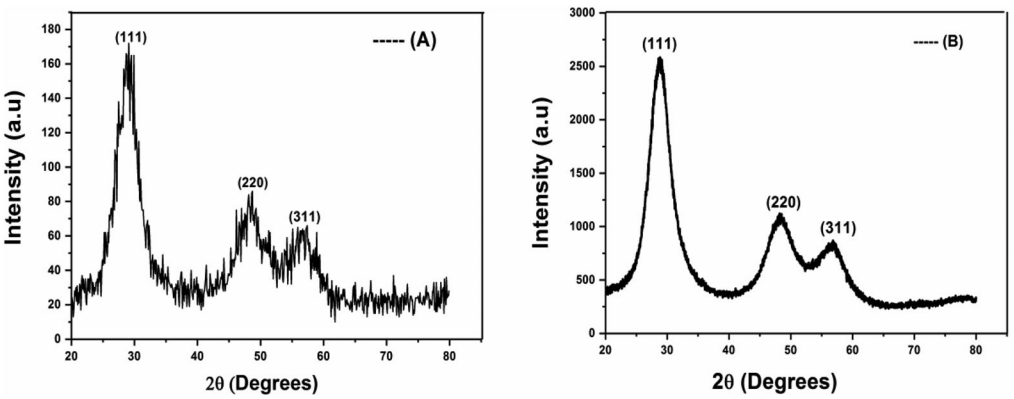

Figure 1. XRD images of (A) pure and (B) Cu-doped ZnS nanopowders.

3. Results and discussions

3.1. Structural analysis

Structural properties of pure and doped ZnS nanopowders are studied with powder XRD technique. Figure 1 shows arrays in peaks of ZnS nanopowders. The three most favored orientations (1 1 1), (2 2 0) and (3 1 1) are detected from this figure, and those peaks show cubic blende structure. These peaks are noticed with XRD shapes and matched well with JCPDS Card No. (80-0020). The XRD array of ZnS nanopowder shows the expansion of the peaks, which specifies the cubic structure of the samples. Debye–Scherrer's formulation is used to calculate the size of the particles [21].

$$D = \frac{0.91\ \lambda}{\beta \cos\theta}$$

where D is the average particle size, λ is the wavelength of Cu Kα radiation, β is the full width at half maximum intensity of the diffraction peak, and θ is the diffraction angle for cubic ZnS. From the XRD calculations, the average size of nanoparticles is in the range of 2–3 nm.

3.2. SEM-EDAX investigations

The spherical shape and morphology of pure and doped nanopowders are examined with SEM. Figure 2 noticed that pure and doped ZnS powders are agglomerated and appears to be nearly spherical in nature. SEM micrographs show the decrease of particles agglomeration with PVP capping agent. The elemental composition has been confirmed by EDAX. Figure 2 displays EDAX spectra of the pure and doped ZnS. This investigation exposes the existence of S, Cu and Zn in prepared powders.

3.3. TEM, HRTEM and SAED analysis

The TEM analysis is also performed to confirm the nanocrystalline nature and to study the morphology of pure and doped ZnS nanoparticles. So morphology and the shape of pure and doped ZnS nanocrystalline powders were confirmed and approved by HR-

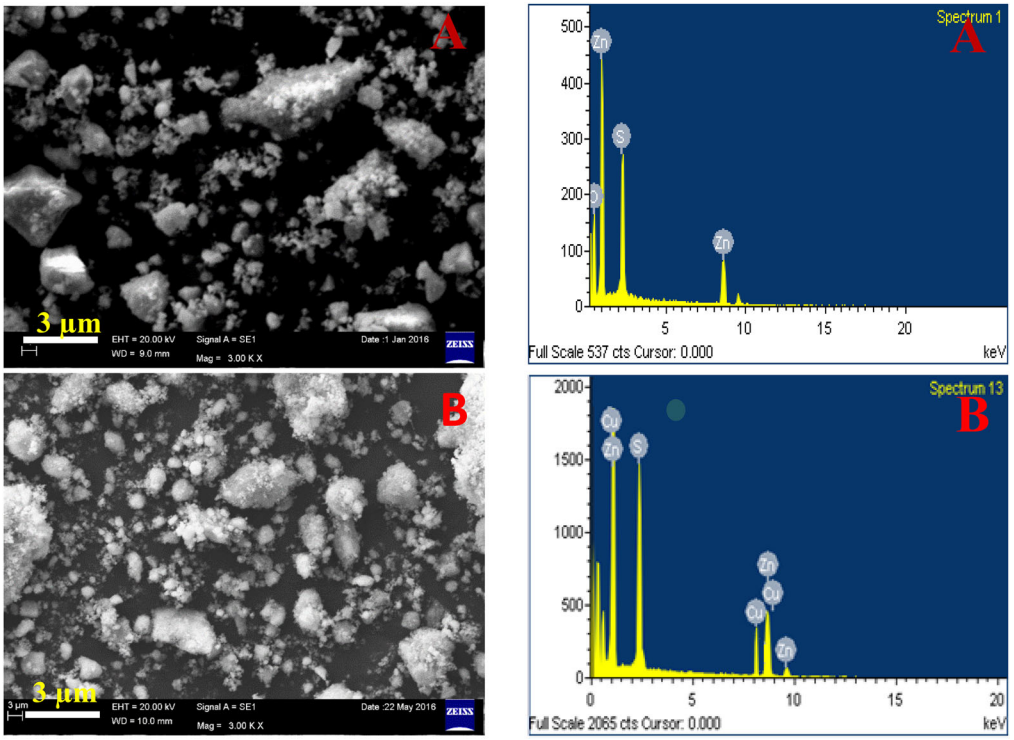

Figure 2. SEM and EDAX images of pure and Cu-doped ZnS nanopowders.

TEM and TEM analysis. SAED, HR-TEM and TEM imageries of Cu: ZnS are shown in Fig. 3. In all the powder particles, the crystallites are isolated and spherical in nature. From the SAED micrographs, it is observed that Cu: ZnS powders of whole concentrations show cubic blended structure with Miller planes (111), (220) and (311). The presences of any secondary phase of Cu collections have not been detected in the XRD and TEM images.

3.4. Photoluminescence analysis

The photoluminescence (PL) spectroscopy is one of the most important tools to investigate the physical properties of ZnS nanoparticles, and the spectra depend upon synthesis conditions, shape, size and energetic position of the surface states [22–24]. From Fig. 4, it can be seen that the 466 nm intensity peak for pure ZnS is associated with natural defects like sulfur vacancy. Additional defect peaks appear in ZnS nanopowders by Cu doping. The PL spectra show sharp emission peaks between 400 and 520 nm. It is in good agreement with previous reports for Cu-doped ZnS nanopowders [25–28]. The emission peaks are observed in the blue region, at 466 [29], 480 [30] and 490 nm [26–28], increases from the recombination among narrow donor level and t_2 level of Cu^{2+} ions [30]. By increasing Cu concentration, the green peaks have systematically moved to longer wavelengths side [31]. Xu [32] observed the PL studies in Cu-doped zinc sulfide nanopowders and perceived green and blue emissions at 519 and 467 nm. Green emission peak is observed by Huang et al. [33] and Sun et al. [34] at 520 nm in

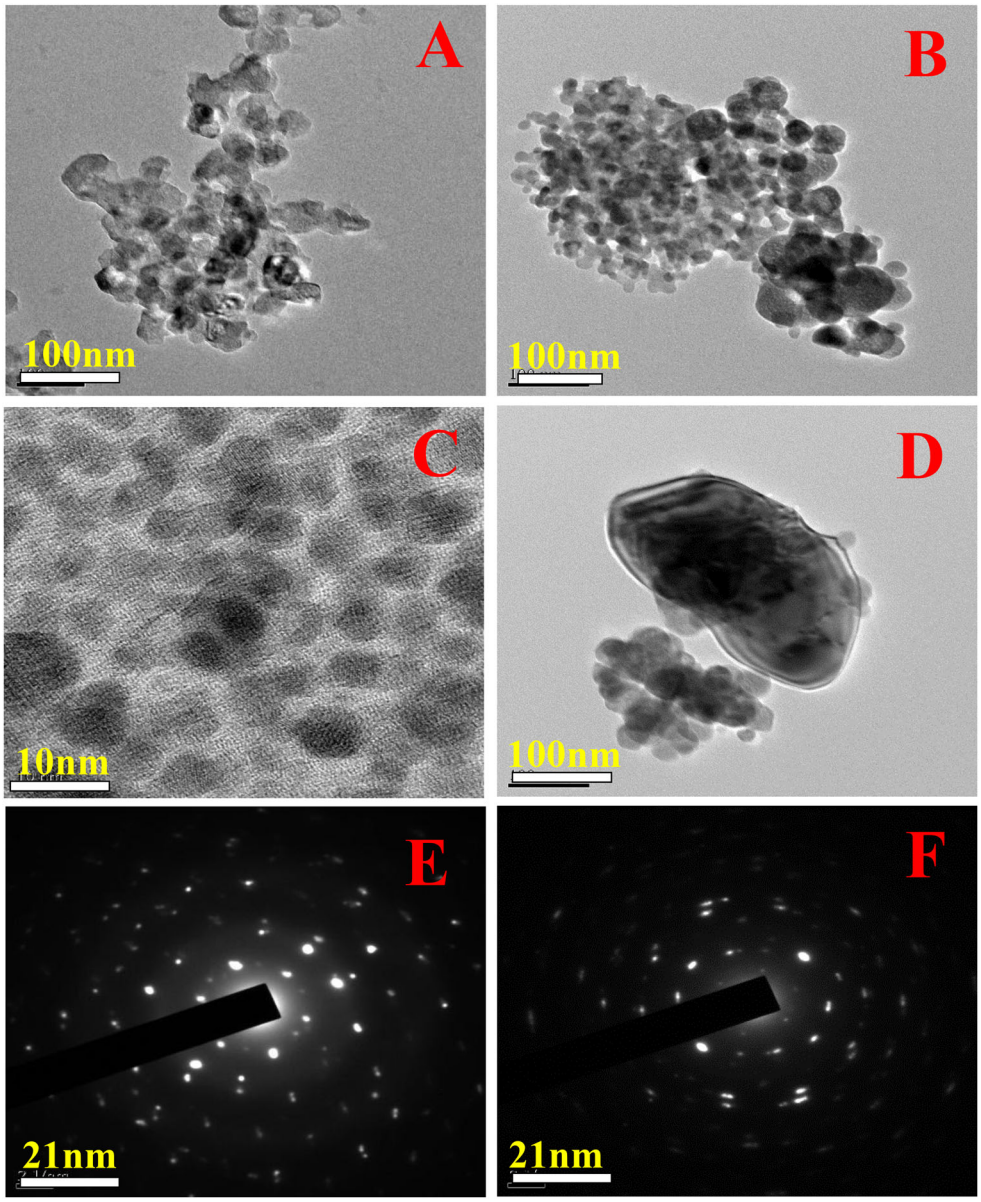

Figure 3. TEM, HR-TEM and SEAD images of pure and Cu-doped ZnS nanopowders.

Cu-doped ZnS nanopowders. Chestnoy et al. [35] similarly observed emission peaks in uv-visible region by Cu-doping into ZnS nanopowders.

3.5. Optical absorption

Figure 5 shows UV-Visible absorption spectra, which investigates the impurity defects in pure and doped Zinc sulfide nanopowders. The optical absorption peak is centered

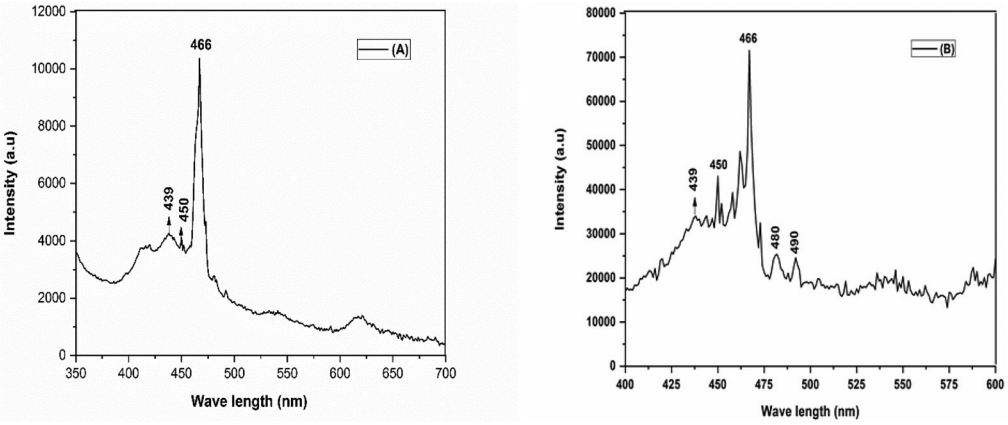

Figure 4. Photoluminescence images of (A) pure and (B) Cu-doped ZnS nanopowders.

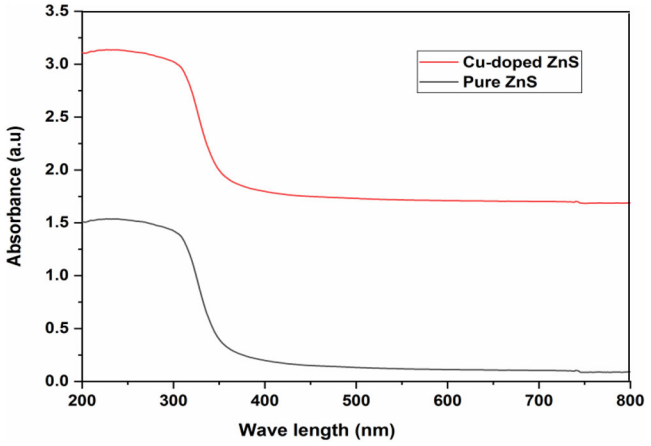

Figure 5. Luminescence Absorption spectra of pure and Cu-doped ZnS nanopowders.

at 310−320 nm for pure and doped samples. As particle size decreases, blue-shifting is observed in doped Zns, and it shows a small change in position with increasing concentration. In pure and Cu-doped samples, absorption peaks are considerably blue-shifted from ZnS with decreasing particles size in nanometers scale and is the quantum effect [36].

4. Conclusion

Pure and Cu-doped ZnS nanoparticles were synthesized using the chemical co-precipitation method. From XRD studies, the synthesized nanopowders show a cubic blended structure. Shape and chemical compositions of all synthesized samples are examined by SEM and EDAX images. Pure and doped nanopowders show UV-optical absorption at

310–320 nm. PL studies show emission peaks are in the visible region. The TEM images show that the shape of pure and doped ZnS nanopowders is spherical in nature.

References

[1] S. A. Wolf *et al.*, Spintronics: A spin-based electronics vision for the future, *Science* **294** (5546), 1488 (2001). DOI: 10.1126/science.1065389.

[2] J. S. Kim *et al.*, Self-assembled hybrid nanoparticles for cancer-specific multimodal imaging, *J. Am. Chem. Soc.* **129** (29), 8962 (2007). DOI: 10.1021/ja073062z.

[3] Y. Lin *et al.*, Multifunctional composite nanoparticles: Magnetic, luminescent, and mesoporous, *Chem. Mater.* **18** (22), 5170 (2006). DOI: 10.1021/cm061976z.

[4] S. Santra *et al.*, Synthesis of water-dispersible fluorescent, radio-opaque, and paramagnetic CdS:Mn/ZnS quantum dots: A multifunctional probe for bioimaging, *J. Am. Chem. Soc.* **127** (6), 1656 (2005). DOI: 10.1021/ja0464140.

[5] N. Banerjee, and S. B. Krupanidhi, Facile hydrothermal synthesis and observation of bubbled growth mechanism in nano-ribbons aggregated microspherical Covellite blue-phosphor, *Dalton Trans.* **39** (41), 9789 (2010). DOI: 10.1039/c0dt00386g.

[6] H. C. Ong, and R. P. H. Chang, Optical constants of wurtzite ZnS thin films determined by spectroscopic ellipsometry, *Appl. Phys. Lett.* **79** (22), 3612 (2001). DOI: 10.1063/1.1419229.

[7] Y.-C. Fang *et al.*, Effects of the S/Zn Ratio on the Photoluminescence Properties of Color-Tunable ZnS:Mn Nanophosphors, *J. Electrochem. Soc.* **156** (4), k55 (2009)., DOI: 10.1149/1.3079621.

[8] S. Kar, and S. Biswas, White light emission from surface-oxidized manganese-doped ZnS nanorods, *J. Phys. Chem. C.* **112** (30), 11144 (2008). DOI: 10.1021/jp800181r.

[9] Z. Quan *et al.*, Multicolor tuning of manganese-doped ZnS colloidal nanocrystals, *Langmuir* **25** (17), 10259 (2009). DOI: 10.1021/la901056d.

[10] S. S. Thilo, M. Ullrich, and F. Rainer, *Nano Lett.* **9**, 453 (2009).

[11] S. Sapra *et al.*, Emission properties of manganese-doped ZnS nanocrystals, *J. Phys. Chem. B.* **109** (5), 1663 (2005). DOI: 10.1021/jp049976e.

[12] W. Q. Yang *et al.*, Color tuning of photoluminescence from ZnS nanobelts synthesized with Cu and Mn doping and without intentionally doping, *Phys. Lett. A.* **372** (27-28), 4831 (2008). DOI: 10.1016/j.physleta.2008.05.009.

[13] T. Kang *et al.*, Synthesis and magnetic properties of single-crystalline Mn/Fe-doped and co-doped ZnS nanowires and nanobelts, *J. Phys. Chem. C.* **113** (14), 5352 (2009). DOI: 10.1021/jp808433b.

[14] S. Bhattacharya, and D. C. Chakravorty, Electrical and magnetic properties of cold compacted iron-doped zinc sulfide nanoparticles synthesized by wet chemical method, *Chem. Phys. Lett.* **444** (4-6), 319 (2007). DOI: 10.1016/j.cplett.2007.07.040.

[15] S. S. Nath *et al.*, Green luminescence of ZnS and ZnS:Cu quantum dots embedded in zeolite matrix, *J. Appl. Phys.* **105** (9), 094305 (2009). DOI: 10.1063/1.3110767.

[16] J. H. Park *et al.*, White-electroluminescent device with ZnS:Mn, Cu, Cl phosphor, *J. Lumin.* **126** (2), 566 (2007). DOI: 10.1016/j.jlumin.2006.10.012.

[17] X. R. Yu *et al.*, Auger parameters for sulfur-containing compounds using a mixed aluminum-silver excitation source, *J. Elect. Spectrosc. Relat. Phemom.* **50** (2), 159 (1990). DOI: 10.1016/0368-2048(90)87059-W.

[18] L. Sun *et al.*, ZnS nanoparticles doped with Cu(I) by controlling coordination and precipitation in aqueous solution, *J. Mater. Chem.* **9** (8), 1655 (1999). DOI: 10.1039/a903761f.

[19] A. Datta, K. Panda, and S. Chaudhuri, Phase transformation and optical properties of Cu-doped ZnS nanorods, *J. Solid State Chem.* **181** (9), 2332 (2008). DOI: 10.1016/j.jssc.2008.05.037.

[20] S. Sambasivam *et al.*, ESR and photoluminescence properties of Cu doped ZnS nanoparticles, *Spectrochimica Acta A* **71** (4), 1503 (2008). DOI: 10.1016/j.saa.2008.05.009.

[21] H. Abdullah, and S. A. Halim, Electrical and microstructural properties of $(La_{1-x}Pr_x)_{1/2}Ba_{1/2}MnO_3$ compounds, *Sains. Malay* **23**, 213 (2009).
[22] W. Chen *et al.*, Absorption and luminescence of the surface states in ZnS nanoparticles, *J. Appl. Phys* **82** (6), 3111 (1997). DOI: 10.1063/1.366152.
[23] T. Arai, T. Yoshida, and T. Ogawa, *J. Appl. Phys* **62**, 396 (1987).
[24] M. Agata *et al.*, Photoluminescence spectra of gas-evaporated CdS microcrystals, *Solid State Commun* **76** (8), 1061 (1990). [Database] DOI: 10.1016/0038-1098(90)90084-O.
[25] S. J. Xu *et al.*, *Appl. Phys. Lett* **72**, 478.
[26] P. H. Borse *et al.*, *J. Mater. Sci* **34** (24), 6087 (1999). [Database] DOI: 10.1023/A:1004709601889.
[27] M. Wang *et al.*, Synthesis and optical properties of ZnS:Cu(II) nanoparticles, *Solid State Commun.* **115** (9), 493 (2000). [Database] DOI: 10.1016/S0038-1098(00)00218-0.
[28] H. Weller *et al.*, Photochemistry of colloidal metal sulfides. 7. Absorption and fluorescence of extremely small ZnS particles (the world of the neglected dimensions), *Ber. Bunsenges Phys. Chem.* **88** (7), 649 (1984). DOI: 10.1002/bbpc.19840880715.
[29] H. Wang *et al.*, Preparation and characterization of ZnS:Cu/PVA composite nanofibers via electrospinning, *Mater. Lett.* **60** (20), 2480 (2006). DOI: 10.1016/j.matlet.2006.01.021.
[30] A. A. Khosravi *et al.*, Green luminescence from copper doped zinc sulphide quantum particles, *Appl. Phys. Lett.* **67** (18), 2702 (1995). DOI: 10.1063/1.114298.
[31] S. Lee *et al.*, Effects of synthesis temperature on particle size/shape and photoluminescence characteristics of ZnS:Cu nanocrystals, *Mater. Lett.* **58** (3-4), 342 (2004). DOI: 10.1016/S0167-577X(03)00483-X.
[32] X. Xu, *Solid Luminescence* (Chinese Academy of Science and University of Science and Technology, China, 1996).
[33] J. Huang *et al.*, Photoluminescence and electroluminescence of ZnS:Cu nanocrystals in polymeric networks, *Appl. Phys. Lett.* **70** (18), 2335 (1997). [Database] DOI: 10.1063/1.118866.
[34] L. Sun *et al.*, Optical properties of ZnS:Cu colloid prepared with sulfurous ligands, *Solid State Commun.* **111** (9), 483 (1999). DOI: 10.1016/S0038-1098(99)00246-X.
[35] N. Chestnoy *et al.*, Luminescence and photophysics of cadmium sulfide semiconductor clusters: the nature of the emitting electronic state, *J. Phys. Chem.* **90** (15), 3393 (1986). [Database] DOI: 10.1021/j100406a018.
[36] A. Deshpande *et al.*, Interfacial and physico-chemical properties of polymer-supported CdS·ZnS nanocomposites and their role in the visible-light mediated photocatalytic splitting of water, *J. Colloid Interface Sci.* **333** (1), 263 (2009). DOI: 10.1016/j.jcis.2009.01.037.